

# EXAMINATION OF THREE-DIMENSIONAL EFFECTS OF INTERNAL EROSION (IE) AND PIPING PROCESSES IN SOIL

Scott Anderson, P.E., National Technology Leader for Numerical Modeling<sup>1</sup>  
Keith Ferguson, P.E., National Dam and Hydraulic Structures Practice Leader<sup>2</sup>

## ABSTRACT

Internal erosion and piping is one of the primary causes of failure of embankment dams. However evaluating seepage conditions that could lead to the development of this potential failure mode is a difficult task and requires understanding of the processes associated with soil erosion, extensive experience, and keen engineering insight and judgment. Two dimensional seepage models, while providing valuable information, cannot adequately model backward erosion and piping phenomenon. This paper takes a look at the current understanding of internal erosion (IE) processes and mechanisms, and discusses the importance of three dimensional effects on the assessment of these processes in soils susceptible to erosion. The paper includes a re-examination of the laboratory testing and three dimensional modeling research conducted by the University of Florida on defect propagation that became the basis of Schmertmann's methodology for estimating factor of safety against piping (Schmertmann, 2000). The previous numerical models are updated using modern 3-D seepage models to take a closer look at seepage gradients and flow concentration that may develop at, and near the active face (upstream end) of the defect. In addition, a 3-D model of a layered system is presented and compared to the 2-D modeling results and observations of a seepage defect that developed at Isabella dam (CA). Results from these two and three dimensional seepage models will be presented and compared, providing practical guidance on the evaluation of erosion/piping failure modes in embankment dams. Three dimensional effects at the entrances to defects in outlet conduits, bedrock openings and at contacts with coarse materials that cannot filter finer erodible soils are also discussed.

## INTRODUCTION

The process and mechanisms of internal erosion are a key area of emphasis within the dam and levee engineering community in the US and around the world. The ongoing research and documentation that is occurring are summarized in the following sections to establish a framework for the later discussion of the importance of 3-D effects when assessing potential internal erosion failure mechanisms, particularly in foundation soils immediately below the base of an embankment dam.

---

<sup>1</sup> HDR Engineering, Inc., 1670 Broadway, Suite 3400, Denver, CO 80202, 303-764-1520,  
[scott.t.anderson@hdrinc.com](mailto:scott.t.anderson@hdrinc.com)

<sup>2</sup> HDR Engineering, Inc., 1670 Broadway, Suite 3400, Denver, CO 80202, 303-764-1520,  
[keith.ferguson@hdrinc.com](mailto:keith.ferguson@hdrinc.com)

**The Importance of Internal Erosion Failure Modes.**

ICOLD (Bulletin 164, 2013), and Chapter 26 of the USBR/USACE Best Practices for Dam and Levee Safety Risk Analysis documents provide excellent summaries of both failures and internal erosion incidents associated with embankment dams. Much of these summaries are derived from the work of Foster and Fell documented in a variety of references beginning in about 1998, as well as Engemoen (et. al.) at the U.S. Bureau of Reclamation beginning in about 2009. A few excerpts from these documents indicating the relative importance of IE to other potential failure modes are provided in Tables 1 and 2, below.

As can be seen in Table 1, 46 percent of all embankment dam failures can be attributed to internal erosion processes. Table 2 further indicates that 67 percent of internal erosion failures occur within the embankment dam and the remaining 33 percent occur within the foundation. Nearly one half of the failures within the embankment were associated with conduits which penetrate, or walls which support the embankment.

Table 1 – Overall Statistics of Embankment Dam Failures

Failure Mechanism	Erosion		Embankment Sliding	
	External erosion (overtopping)	Internal erosion	Static Instability	Seismic instability
% over the world	48%	46%	4%	2%
% over the world	94%		6%	

Table 2 – Further Statistics of Embankment Dam Failures through the Embankment or Foundation

No. of Cases		% of Failures (if Known)		Average Probability of Failure	
All Failures	Failures in Operation	All Failures	Failures in Operation	All Failures	Failures in Operation
<b>Internal Erosion through the Embankment</b>					
39	38	30	33	3.5E-03	3.5E-03
<b>Internal Erosion through the Foundation</b>					
19	18	15	15	1.5E-03	1.5E-03

Both Redlinger and Engemoen, on behalf of the U.S. Bureau of Reclamation have recently carried out detailed analyses of internal erosion incidents at 220 of Reclamations dams (ICOLD, 2013). It is important to note that this portfolio of dams generally represent 1) a subset of the entire US portfolio designed and constructed within a single agency and their engineering practice guidelines and 2) relatively large structures that are usually filled to ‘normal “high” pool levels’ (within 7 to 12 feet of the dam crest) at the beginning of each year. ICOLD notes that the definition of “incident” in this assessment is not the same as the ICOLD definition. The Reclamation findings are as follows:

- 99 of the 220 embankment dams had experienced incidents (45%)
- Of these 99 incidents, 1 was a failure, 53 involved definite particle transport, and the remaining 45 were excessive seepage or sand boils.
- Of these 99 incidents, 9 occurred in the embankment, 70 in the foundation, 6 from the embankment into a conduit, 5 were into or along a conduit, and 11 were into a toe or under drain.

### **Internal Erosion Mechanisms**

The following is a summary of internal erosion mechanisms that are currently in use in the dam and levee engineering community of practice within the US and internationally (USBR/USACE Best Practices, Chapter 26, 2014; ICOLD, bulletin 164, 2013; Authors experience).

- *Piping* (Backward erosion piping (BEP)) – Occurs when soil erosion begins at an unfiltered seepage exit and continues its way upstream through the embankment, foundation, or both, forming a continuous pathway toward the reservoir . Two primary physical “erosion” *processes* are present in this overall mechanism; 1) adequate seepage gradients and flow quantities (energy) for **detachment** particles within the active erosion front (pipe head), and 2) once a particle is detached, adequate flow quantity and velocity in open “pipes” to **transport** eroded soils through the forming defect. In addition to these erosion processes several other conditions must be present for this overall mechanism to continue (progress) toward and open into a reservoir:
  - 1) a continuous flaw or pathway for the “pipe” to develop. Note that different types of flaws can connect to form one continuous flaw,
  - 2) relatively permeable and erodible material within the flaw/flow path (fine sand, silty sands, and sandy silts), and
  - 3) conditions allowing for the formation of a stable and open “pipe” downstream of the active front. Typically, this is described as a “roof”.

In general, recent publications suggest that this mechanism is controlled primarily by horizontal gradients and seepage flows. As will be subsequently demonstrated, idealized 3-D seepage models suggest that within the active seepage “front” within a developing “pipe” (typically two or more diameters from the active “face” or pipehead), the gradient and velocity vectors are highly variable ranging from horizontal to vertical and both component likely influence the erosion process. This confirms some of the original observations by Townsend (1981) and Schmertmann (2000) and suggests that **detachment** is a highly complex process with important contributions from vertical gradients typically associated with a “heave” or “quick” condition described below, horizontal gradients, and the actual quantity of flow entering the pipe at that quantities ability to transport the detached particles from the active erosion region.

- *Stopping* (Internal migration) erosion – Particle movement is driven by gravity in materials that are not capable of sustaining a roof or pipe. It is characterized by the formation of localized voids that successively grow and collapse leading to the formation of sinkholes, and localized over-steepening of embankment slopes leading to progressive instability.

- *Heave or Quick condition* (sand boils) – The original pioneering work on this issue was performed by Terzaghi at Robert College, Bebek, Turkey beginning in about 1918. Terzaghi’s experiments showed that as upward hydraulic forces through a column of sand were increased, “the quantity of percolation would increase proportionally (in accordance with Darcy’s Law) until the upward hydraulic force became equal to the submerged weight of the column of sand. Then the flow would immediately and dramatically increase while the sand underwent a complete change in its fabric, acquiring a very loose grain packing. In other words, the structure of the sand had rearranged itself automatically into a looser and much more permeable fabric in order to reestablish hydraulic equilibrium between the weight of the sand and the now much smaller force of the flowing water.” (Goodman, 1999). Terzaghi subsequently constructed model dams, of various shapes, and observed the effects of gradually raising the water level stored behind them. As the water height increased, a critical height would be reached at which sand on the submerged surface at the downstream toe of the dam would appear to “boil” as it suffered erosion of fine particles; shortly afterwards, a tunnel would be eroded completely under the dam, and the reservoir would summarily wash through it – a classical failure by “piping”. This critical height was perfectly computed from the hydraulic flux and permeability at the worst point along the seepage path, which was usually at the downstream toe of the dam.
- *Uplift and Blowout* – This mechanism can occur if the embankment or a confining, low permeability foundation layer overlies a more permeable layer under and at the downstream toe of an embankment. Under this condition relatively high (artesian) water pressures may develop at the base of the embankment/confining layer. When these pressure become higher than the submerged weight of the confining layer materials the confining layer is “lifted” upwards resulting in the formation of cracks providing an unfiltered pathway for the erosion (blowout) of the higher permeability soils below the confining layer.
- *Concentrated leak erosion* – Involves and erosion mechanism along the edges or perimeter of an opening (crack or pipe) in which concentrated leakage is occurring. This is sometimes referred to as “scour” and is related to **contact erosion** (ICOLD, 2013, USBR/USACE, 2012). The primary erosion mechanism at work is associated with the removal of soil at the exposed face or surface of the defect due to concentrated water flow in the defect. This type of erosion mechanism has typically be the subject of research associated with river mechanics and scour and authors such as Hjulstrom, 1935; Ishbash, 1936; Briaud, 2007, and others provide excellent research results that can inform our understanding of internal erosion when the primary erosion mechanism is concentrated flow within a defect. This mechanism is at work during the gross enlargement stage once a continuous pipe or defect (crack) has reach an open source of water such as a highly permeable shell, open joint, or the reservoir.
- *Suffusion* – Selective erosion of finer particles from the matrix of coarser particles, leaving behind a soil skeleton. Because the coarser particles carry stresses within the soil, little to no loss of matrix integrity or change in volume occurs. It is interesting to note that this phenomenon was referred to as “scour” by Terzaghi when evaluating the

left abutment seepage at Cleveland Dam in British Columbia (Goodman, 1999). Later, Sherard called this phenomenon “internally unstable gradings” (Sherard, ).

- *Suffosion* – Similar to suffusion except effective stress is carried by the finer fraction and movement of these fines results in a reduction in the total volume and collapse of the soil matrix.

### Internal Erosion Stages

The following is a summary of the stages of internal erosion that are generally used in the US and throughout the world when performing potential failure modes and risk assessment activities for embankment dams (ICOLD bulletin 164, 2013, Authors experience). Some additional clarifications of the stages are presented. The Author’s note that these stages may involve very different considerations and factors for different potential failure pathways through a dam verses through the dam foundation. Much of the literature today provides a somewhat ambiguous differentiation between the “continuation” and “progression” stages. The Authors offer a more definitive definition based on the specific erosion mechanisms at work in the overall erosion process.

- *Initiation* – Initiation is the time and location where erosion begins at a point of seepage discharge:
  - 1) from an unfiltered defect, geologic anomaly, or crack along the downstream toe of embankments,
  - 2) at defects in conduits, drain systems, and along structures;
  - 3) at location(s) of filter incompatibility at zone contacts in embankments, within foundations, and at the contact between the embankment and foundation;
  - 4) at location(s) of concentrated leakage discharge from an embankment/foundation crack due to differential settlement or hydraulic fracturing (Sherard, 1985; McCook and Grotrian, 2010; Ferguson et al, 2013); and
  - 5) from the embankment into foundation defects such as open joints, and karst features.
- *Continuation* – the portion of the piping and erosion mechanism where internal erosion is governed by **detachment** and **transport** processes. Seepage into developing defects and the corresponding detachment and transport of soil during this stage is controlled by the location and characteristics of the flaw (pathway dimensions, coefficient of uniformity ( $C_u$ ) and permeability of the soil surrounding the defect, ability to form a roof, etc.). During this stage, developing pipes remain relatively small and difficult to detect unless other mechanisms such as stoping and sinkhole development occur as part of the IE process (e.g. Ferguson, et. al., 2014).
- *Progression* – the portion of the piping and erosion process where significant gross enlargement occurs and erosion is governed by **concentrated leak erosion** (also referred to as “**scour**”) processes. The rate of erosion is controlled by the erodibility of the embankment/foundation soils at the surface of the defect when exposed to flowing water

within the defect. Other considerations related to the progression stage include the ability of 1) embankment zoning (coarser shell materials) or conditions within a foundation defect (e.g. the walls of a joint or karst feature) that could limit or terminate the growth of the defect, 2) material characteristics (dispersion), or 3) the potential for embankment or foundation material to collapse, swell, or otherwise self-heal (such as development of a natural filter) along the erosion pathway.

- *Breach formation* – The gross enlargement process is completed during this stage resulting in the uncontrolled release of the reservoir.

### **Factors Influencing the Internal Erosion (Piping) Processes**

The following is a summary of the factors influencing the internal erosion (piping) process as discussed by a number of noted researchers including Townsend, Schmertmann, USBR, Fell et al (2008), ICOLD bulletin 164, Hjulstrom (1935, 1956), Briaud (2007).

- Particle **Detachment** (at unfiltered discharge)
  - ✓ The primary factors influencing detachment include 1) particle size and size distribution (coefficient of uniformity), 2) seepage gradients/velocity/energy at the active front, and 3) soil density/stress state.
  - ✓ Townsend et. al. (1988) observed the following from the University of Florida piping flume tests: “Piping begins to form with the displacement of several sand particles at the tip of the initial pipe. The particles slide into the newly created channel, and when finally washed away, several more new particles became displaced as a retrogressive slide. A continuous landslide and erosion process exists which propagates the pipe. However for sand with large grain sizes or large coefficients of uniformity,  $C_u$ , insufficient water velocities exist to erode the soil particles after they slide into the initial pipe and deposition may occur downstream in the pipe. Because of this deposition, the piping may be retarded or even ceased by self-healing.”
- Particle **Transport** and Deposition (sedimentation)
  - ✓ Particle size, size distribution, and specific gravity
  - ✓ Flow velocity in the defect, depth, and velocity variations within system of developing defects
  - ✓ Other factors contributing to a transition from erosion to deposition within a defect
- **Concentrated Leak Erosion (Scour)** – gross enlargement processes
  - ✓ Particle size and specific gravity, shear stress, flow velocity in the defect

### **Key Factors In Assessing Dam Safety Risks Associated with Internal Erosion**

Based on the authors experience investigation and assessing seepage failure modes (both incidents and actual failures), the following is a summary of the most significant considerations associated with each stage of the seepage failure mode process:

- Initiation
  - ✓ The potential for an unfiltered natural or man-made defect that would result in the concentration of seepage gradients and flows that could cause initiation of particle migration

- Continuation and Progression/gross enlargement
  - ✓ The potential for a continuous pathway (layer, crack, hydraulic fracture or other natural or man-made defect from the point of initiation to the reservoir or water source)
  - ✓ The permeability of the soils and ability to generate adequate seepage quantity and velocity (energy) to **detach and transport** the full range of soil particle sizes along the pathway
  - ✓ The erodibility of the soils along the pathway (coefficient of uniformity,  $C_u$ ; plasticity, density/specific gravity)
  - ✓ Conditions that promote the stability of the piping feature (roof or pipe channel)
  - ✓ Conditions that could arrest the advancement of the piping/erosion feature such as changes in material type along the pathway, collapse, and development of a natural filter. Natural filters may develop in the presence of more widely graded soils and sufficient energy only to transport a portion of the gradation, leaving coarse materials deposited in the pipe that eventually cause a natural filter to develop.
- 2-D versus 3-D influences
  - ✓ Once initiation has occurred, seepage conditions at the advancing face (head) of the pipe change dramatically with significant concentration of seepage gradients, flow quantities and velocity.
  - ✓ If initiation is suspected, consideration of 3-D seepage influences on the fundamental factors of detachment and transport become the primary consideration in estimating the likelihood that the continuation process will advance all the way to the reservoir. Methods of assessment that rely on global or point gradients using 2D flow nets or experimental test results are likely not conservative and hence may not be suitable in estimating risk if an initiating event has occurred or is suspected.

### **Using Numerical Models to Inform Understanding of Internal Erosion Processes**

Two-dimensional (2D) versus Three-dimensional (3D) Modeling. Pioneering work on internal erosion process including the development of laboratory test equipment and procedures that allow for the observation of internal erosion processes has been performed at the University of Florida, and the Technical University in Delft. The results of this research were first published in 1981 by Townsend, (et. al.), and in 1988 by Sellmeyer. The work at the University of Florida was triggered by the Martin Plant Dike failure (Florida Power and Light Company), and the authors noted the following as one of the primary basis for their research:

“The theory (*summarized in the report*) is based upon the observation that the horizontal seepage velocities of water flowing through soils are insufficient by one or more orders of magnitude to cause erosion; e.g. piping. Consequently, an additional factor must be present. It is theorized that a significant vertical gradient exists causing the soil grains to become quick; and thus the seepage velocity required for scour approaches zero, making possible the progressive erosion of the pipe. Intuitively, the vertical gradients will become concentrated at the head of the advancing pipe thereby contributing to the pipe’s advance. Dr. Schmertmann quantified the vertical gradients at a pipe tip based upon sketching of flow nets, and related these vertical gradients to the average gradient via a

concentration factor, i.e.  $i_{(vert)} = C \times i_{(ave)}$ , where  $i_{(vert)}$  = perpendicular (vertical) gradient at pipe tip,  $C$  = concentration factor, and  $i_{(ave)}$  = average hydraulic gradient (total head difference/total linear flow distance). The development of these correction factors to account for **three-dimensional** flow into an advancing pipe was limited by flow net sketching, and refinement became an objective of this project... Specifically, the concentration factor values were to be refined using numerical programs and extended for a variety of conditions. Physical model tests were to be performed to verify theoretical concepts concerning the mechanisms of piping and to provide physical data for verifying concentration factor values.”

On the other hand, Sellmeyer notes the following as one of the fundamental bases for his initial research:

‘The whole mechanism (*piping as a form of seepage erosion*) is quite complex and use is made of branches of soil mechanics (both continuum approaches and particulate aspects), groundwater flow and hydraulics. A certain amount of simplification has to be introduced so as to make the problem suitable for mathematical analysis. Inspiration is drawn from simple visual tests... The model is essentially **two-dimensional**. It is believed that this does not seriously affect the validity of the results. The design rules obtained allow for a great variety of geotechnical conditions, The analysis gives insight into the safety factor of the design.”

Recent small-scale experiments have been performed to validate the Sellmeyer’s model for multi-layer aquifers (va Beek, et al, 2012). This study demonstrated that 2D numerical groundwater flow models in which the Sellmeyer numerical model has been implemented (MSEEP) accurately calculated critical heads that were experimentally obtained in small-scale experiments where discharge occurs to a continuous defect (perpendicular to the direction of flow through the models) such as an open channel on the landside of a levee or dike. However, the critical head to initiate erosion into a circular exit point (sand boil) through a confining cover could not be predicted by the 2D numerical program. Subsequent 3D modeling by Vandenboer, et. al. (2014) demonstrated the inherent 3D nature of the piping phenomenon. The authors suggest the superiority of 3D numerical model computations compared to 2D approaches. These authors further suggest that 3D numerical results enable a better understanding of the complex physical mechanisms involved in backward erosion piping and thus can lead to a significant improvement in the safety assessments of water retaining structures.

Ferguson presented information on the 3-D nature of the seepage equipotential and flow lines surrounding the Isabella Auxiliary Dam, CA discharge conduit in 2010 (Ferguson, 2010) based on interpretations of instrumentation readings. The instrumentation readings, along with other observations, and detection of suspected initiation locations in a foundation drain pipe and through defects in the canal lining immediately downstream of the outlet works discharge at Isabella Auxiliary dam suggested that the failure mode process at Isabella Auxiliary Dam had initiated and was in an advanced continuation stage in an erodible silty sand foundation layer adjacent to the outlet conduit excavation. In 2012, Ferguson, et al (2012) presented the results of

2D seepage modeling of a hypothetical defect within an idealized confined and layered foundation built from the observed conditions at Isabella Dam. Results of 2D seepage modeling suggested that exit gradients at all points of an active seepage front within a model defect (including the point of initiation) were likely sufficient to result in the continuation of a piping erosion process beneath the dam, particularly when considering how gradients concentrate around the advancing front (head) of a seepage defect. However, the estimated seepage quantities into the model piping defect (0.001 to 0.01 gallons per minute (gpm) per foot) were not consistent with the observed flow discharging from a drain pipe where the defect initiated (>1 to as much as 7 gpm). Specifically, the estimated seepage quantities for various reservoir levels from the 2D model were likely insufficient to effectively transport detached particles from the active front of the defect. The observed seepage was up to at least 100 times larger than the seepage estimated by the 2D model. At that time, Ferguson et. al., cautioned that the 2D model was a simplification and acknowledged that the actual development of the piping or erosion feature, and the corresponding regime of water pressures (equipotential lines), gradients and flow quantities that would develop in the vicinity of the defect is a three dimensional (3D) problem. Hence, “the actual gradients and flow quantities into the active front and upstream portion of a pipe or erosion defect could be substantially higher than the 2D model results indicate.”

#### REVIEW OF SCHMERTMAN RESEARCH AND FACTOR OF SAFETY METHOD

In response to the October 30, 1979 failure of a portion of the embankment containing a cooling water reservoir at a Florida Power and Light Company power plant, Dr. Schmertmann, a member of a Board of Consultants convened to investigate the cause of failure, developed a theory to assist in analyzing the failure and to investigate the safety of other earth embankments (Schmertmann, 1980). At that time, Schmertmann had noted that only empirical methods and engineering judgment were available for the design of dams/ or to evaluate foundation materials and their resistance to piping. Subsequent to the development of the theory, a research program was initiated at the University of Florida (UF), to help verify and refine Schmertmann’s piping theory.

The seepage research work at the UF first published in 1981 by Townsend et. al. had, as a principal component of the work, the development and use of a 3-D finite element seepage program to examine gradient concentration factors parallel and perpendicular to an internal erosion “pipe” for various pipe penetrations and boundary conditions. The other primary component of the research work included the development and evaluation of an experimental flume to identify the average gradients required to initiate piping, and to observe the piping process.

A 3-D finite element program for seepage written by the US Waterways Experiment Station (WES) was used (Wong, 1981; Tracy, no date) as the basis for the UF research work. The program identified by “SEEP3D” could be used to solve both transient and steady state seepage problems. The UF research used only the steady state formulation. The program at that time had the limitation of permitting a maximum of only 1000 nodal points in the finite element grid. This proved a severe limitation and required some undesirable approximations in interpreting the results (Wong, 1981).

In later advancing his initial theory for evaluating the potential for piping and internal erosion, Schmertmann performed a comprehensive review of the 3-D modeling and laboratory testing procedures and observations at UF, as well as related research performed at the Technical University at Delft (Selljeyer, 1988). Some important observations from the Schmertman paper (2000) are as follows:

- ✓ The term “piping” is defined as the erosion of soil, due to concentrated internal seepage, within a mass of soil, and “scouring” as the erosion along a soil surface due to water flowing along that surface, without the need for seepage through the soil to that surface. He further notes the importance of both seepage gradient and “roof” support conditions to the “piping” erosion process.
- ✓ 3D seepage concentration is required to cause “piping” or for internal erosion to occur. Under normal conditions in a dam foundation, the gradients are not sufficient to cause the initiation or “progression” of piping.
- ✓ Both 2D and 3D flow nets were used to understand the piping phenomenon and inform the factor of safety method presented in the paper. The 3D computer studies by Wong (Townsend, 1981) are noted but it appears that the majority of the assessment method relied on the combining longitudinal, transverse and horizontal section 2D flow nets to estimate 3D conditions.
- ✓ The proposed method in the paper uses an average or global factor of safety as well as the point-by-point variation of the factor of safety vs. piping along a potential pipe path. The global gradient needed for piping to continue in the various experiments at the UF and in Delft varied with the percent downstream-upstream advance of the pipe and reached a maximum at a penetration of 30 to 50 percent in the Delft experiments, and about 20% in the UF tests. This experimental observation is illustrated in the figures below taken from Chapter 26 of the USBR/USACE Best Practices for Risk Analysis. Note the reference to a summary of this phenomenon by Van Beek taken from an article written in 2010. This information appears in work published by various Delft researchers including Sellmeijer from 1981 to 1993 and was reviewed in detail by Schmertmann (2000).

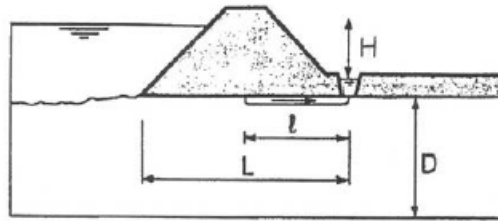


Figure 26-17. Geometry of Delft Backward Erosion Model  
(Weijers and Sellmeijer, 1993)

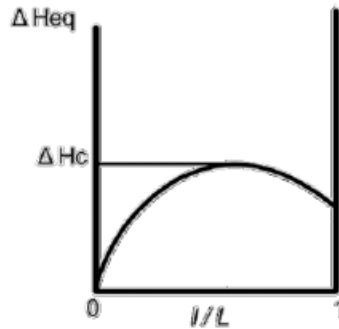
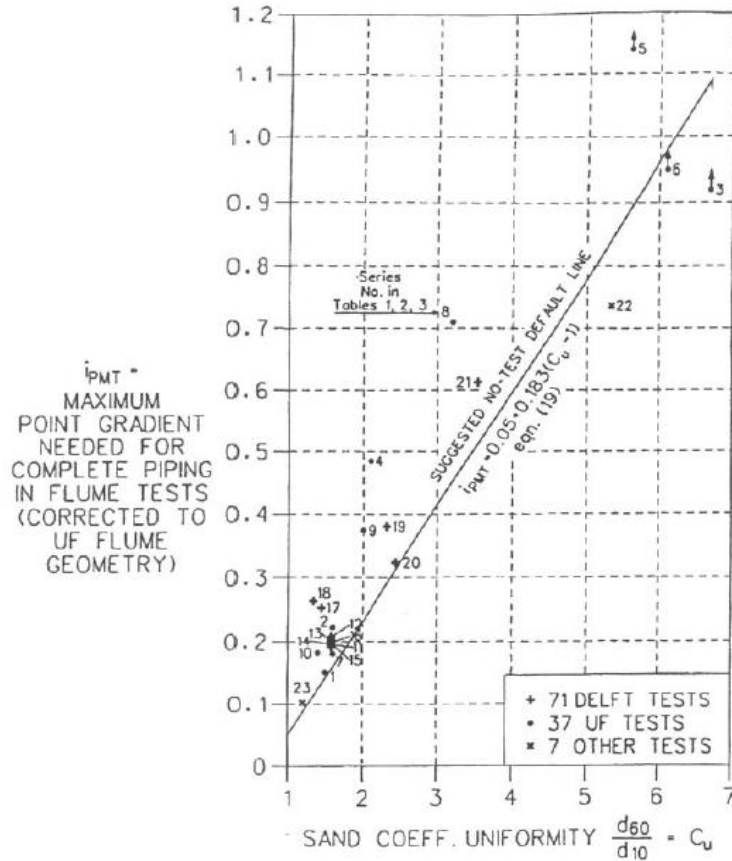


Figure 26-18. Hydraulic Head as a Function of the Ratio between  
Pipe Length and Seepage Length  
(van Beek et al., 2010)

Schmertmann believed that this pattern could be explained from the flow net pattern of equipotential line concentrations associated with the dimensions of the testing equipment and not as a result of a fundamental aspect of the piping phenomenon itself. To utilize the experimental results however, required the use of a horizontal gradient correction factor ( $C_{Gt}$ ) to relate the experimental results to an average gradient calculated using flow nets. In other words, it is necessary to multiply the average or global gradient required to sustain the piping process in the lab tests by the horizontal gradient correction factor to estimate the global gradient that is required for sustaining the piping process that would be compared to flow net calculations:

$$i_{pmt} = i_{pmte} \times C_{Gt} \quad (1)$$

Where:  $i_{pmt}$  = the maximum (m) value of the Global (or average gradient) in a flume test (t) required to sustain downstream to upstream piping (p). It represents the minimum Global gradient needed to complete the piping process from the point of initiation to the reservoir  
 $i_{pmte}$  = the maximum (m) value of the global gradient required to sustain piping in lab experiments. Note that multiplying this experimental value by the correction factor,  $C_{Gt}$  give a constant value of  $i_{pmt}$  at any L.



The figure above shows a summary of all the UF and Delft experimental results with the  $C_{Gt}$  correction applied. Note the limited range of  $C_u$  values in the laboratory experiment samples. Due to concerns about the samples, the relationship shown in this figure should be used with caution and perhaps only for soils with  $C_u$  values that are less than 3.2 ( a very narrow range that is seldom encountered in nature).

- ✓ The paper summarizes the “meandering” nature of the piping phenomenon noting that “the piping channel does not advance in a downstream to upstream straight line. Rather, it advances in a meandering, braded system of channels, sometimes with oxbows, and often with one path clogging and stopping progress followed by a restart of another path”. This is consistent with observations in the Delft research that has noted that “the meandering of the pipes is due to the search for weakness in the granular structure of the sand. It is associated with the non-homogeneity of the sand properties and is therefore not a essential but an added feature of the piping problem.”
- ✓ Schmertmann notes that the flow velocity needed for the piping process is substantially less that the flow velocity required in a concentrated leak to cause “scour” (concentrated leak erosion).
- ✓ The paper summarizes the lack of experimental evidence that initial effective stress state influences the piping pathway but goes on to suggest that the “micro” condition of very low effective stresses along its boundaries (the water/sand erosion interface), may control the piping behavior irrespective of the prior “macro” effective stress. Macro effective stresses may have some effect on the piping process such as changing the cross-sectional area or slope of the pipe, but do not appear to change whether or not piping will occur.

- ✓ Based on the University of Florida experimental results, the influence of a developing pipe on distortion of seepage flow patterns and corresponding water pressures in other portions of the dam were postulated to be relatively small. Specifically, in a homogeneous sand, Schmertmann suggests that the influence of a developing pipe extends no more than 80 radii in any direction from a pipe channel and a half-circular cross-section of the pipe. Put into context, for a 12.5mm pipe radius, the local influence of the pipe would not extend a horizontal or vertical distance of more than 1 meter from the pipe. Of course, anisotropy could have a significant impact on this observation.

Considering all of the factors summarized in the paper, including those noted above, Schmertmann summarized two simplifying mechanisms as primary considerations in the development of his Factor of Safety methodology:

Mechanism 1 – Critical Horizontal Gradients and Regressive Slope Failures

Mechanism 2 - Critical Vertical Gradients and Liquefaction

Both of the simplifying mechanisms considered by Schmertmann involve very low “micro” effective stresses at the active front of the pipe (pipehead). Both were observed to have the potential to capture the essence of the piping problem. Schmertmann chose to use the critical vertical gradient method for a number of reasons including:

- The ease at understanding this mechanism
- Ability to visualize and quantify based on using flownets.
- Mechanism seemed to match, at least qualitatively with testing experience.

Careful study of the 3D pipehead gradients determined by Wong (Townsend, 1981) as well as 2D flownet approximations suggested that:

$$i_{he3} = 1.33 \times i_{ve3} \quad (2)$$

Where :  $i_{he3}$  = the 3D horizontal gradient at the pipehead

$i_{ve3}$  = the 3D vertical gradient at the pipehead

The point-by-point methodology in the paper provides an estimate of a factor of safety ( $F_{px}$ ) verses piping along any postulated failure pathway (x):

$$F_{px} = (i_p/i)_{xf}$$

Where:  $i_{pxf}$  = the gradient at a specific point (x) along a potential piping path in the field (f) that would cause piping (p)

$i_{xf}$  = the estimated actual gradient in the field (f) at the sample point (x) from a 2D flow net

The calculated factor of utilizes the  $I_{pmt}$  from laboratory tests and the application of a range of lab-to-field correction factors. A total of eleven correction factors are described. Through a

number of mathematical refinements, the following equation is the final model for estimating the factor of safety along any hypothetical piping pathway of concern.

$$F_{px} = [(C_D C_L C_S C_K C_Z C_\gamma) i_{pmt} (C_\alpha) / C_R i_f] \times$$

The USBR/USACE Best Practice for Risk Assessment (2012), Chapter 26 notes that Schmertmann (2000) contained several errors which have been correct in the equation below to estimate the critical gradient for particle transport (i.e. to advance a pipe to the reservoir,  $i_{adv}$ ).

$$i_{adv} = (i_{pmt})_{corrected} = [(C_D)(C_L)(C_S)(C_K)(C_Z)(C_\gamma)(C_\alpha) / C_R](i_{pmt})$$

The letter C in these equations denotes a “Correction Factor” with each subscript identifying the factor or variable that can be applied when field conditions vary from the laboratory conditions:

- D = the Depth/Length (D/L) factor
- L = the Length factor
- S = the Grain Size factor
- K = the Anisotropic Permeability factor
- Z = the (high permeability) Underlayer factor
- Gamma = the Density factor
- Alpha = the Pipe Inclination adjustment
- R = the Convergent/Divergent flow factor

In general, while being highly informative about the IE process, there are a number of important observations and considerations related to the use of the model presented by Schmertmann;

- a. The Factor of Safety methodology cannot be easily adopted in today's risk informed decision making process where an engineer and/or organization is faced with making best estimates of the probability of failure associated with different potential seepage failure mode pathways, and also consider uncertainty in the range of critical parameters used in the analysis.
- b. Further, the method is very difficult to apply in complex geologic environments where the continuity of potential erosion pathways, and the variability of material properties and dimensions along that pathway can be substantial and introduce significant uncertainties into the assessment process. The method is severely limited by two important factors: 1) the limited range of materials considered in the laboratory tests, and 2) the limitations associated with the 3D modeling that was performed (number nodes, the graphical interface for presentation and interpretation of results, and the number of study cases analyzed).
- c. The method does not explicitly consider the conditions that develop at the active face of the piping feature once initiation has occurred. These conditions, and the primary detachment and transport mechanisms associated with the horizontal and vertical gradient, velocity vectors, and flow quantities at the active front are only implicitly considered through the  $i_{pmt}$  parameter.

## RESULTS OF THREE-DIMENSIONAL COMPUTER MODELING

### Model Configuration

To further examine and evaluate the influence of 3-D seepage conditions in the formation of a pipe during the internal erosion process, the authors have developed a 3-D seepage model as shown on Figure 4. This model is similar to the 3-D seepage model created as part of the UF research (Townsend, et al, 1981). The results from this model that are presented in this paper are considered introductory and will serve as the starting point for future evaluations. It should be noted that the dimensions shown on Figure 4 are in feet. In general, the Y dimension of the model represents conditions from the upstream ( $Y = 0$ ) to a downstream discharge ( $Y = 100$ ) location. The Z dimension represents the elevation above the bottom of the model. An upper confining layer is located at  $Z = 100$  and the bottom of the model is at  $Z = 0$  feet.

Note that the bottom of the model was set as an impermeable boundary for an initial set of study cases. A lower confining layer boundary was later studied at  $Z = 85$  feet as discussed further below. The X dimension represents the model horizontal dimension and was set with a total width of 200 feet, well in excess of any anticipated 3-D influence of a piping feature based on the results of previous physical and computer modeling investigations. The piping feature included in the model extends from the downstream end at  $Y = 100$ ,  $X = 0$ ; and  $Z = 100$ , along the upper left hand edge (looking downstream). The model is axis-symmetric along the  $X = 0$  boundary. Hence the estimated gradients represent conditions along half of the piping feature but would be expected similar for the other half of the pipe feature not included in the model. However, estimated seepage flow into the pipe in the axis-symmetric model represents only half of what would actually occur. A net average gradient of 1 was applied in the model (similar to the models at UF). Establishing conditions for an applied average gradient of 1 provides a number of numerical conveniences. Perhaps the most important convenience is that actual gradients and flow quantities for conditions where the average gradient is less than 1.0 can be easily obtained by simply multiplying the computer model gradients and/or flow quantities presented in this paper by the average gradient that exists under specific field condition in question. For the Isabella Dam example that will be subsequently discussed, the average gradient is on the order of 0.1 to 0.2, depending on the reservoir level. The computer results can hence, be multiplied by 0.2 to estimate the actual gradient and seepage flow conditions that would ideally occur in the field.

The UF model was limited to 1,000 nodes, resulting in a maximum of 729 elements. As previously noted, the boundary conditions of the UF model were set to generate an average gradient of unity ( $i_{ave} = 1.0$ ), achieved by applying a head of 100 (feet) across a model horizontal dimension L of 100 (feet). The pipe was represented by a triangular shaped void in the mesh. The void "radius" was the length of the sides of the triangle. The radii of  $0.005 \times L$  (0.5 feet or 6 inches) and  $0.01 \times L$  (1 foot) were evaluated as one of the variables explored in their study. A considerable portion of the study was performed to evaluate the influence in the model dimensions on the estimates of seepage gradients entering the void. For the current modeling effort, the final dimensions of the UF model were adopted.

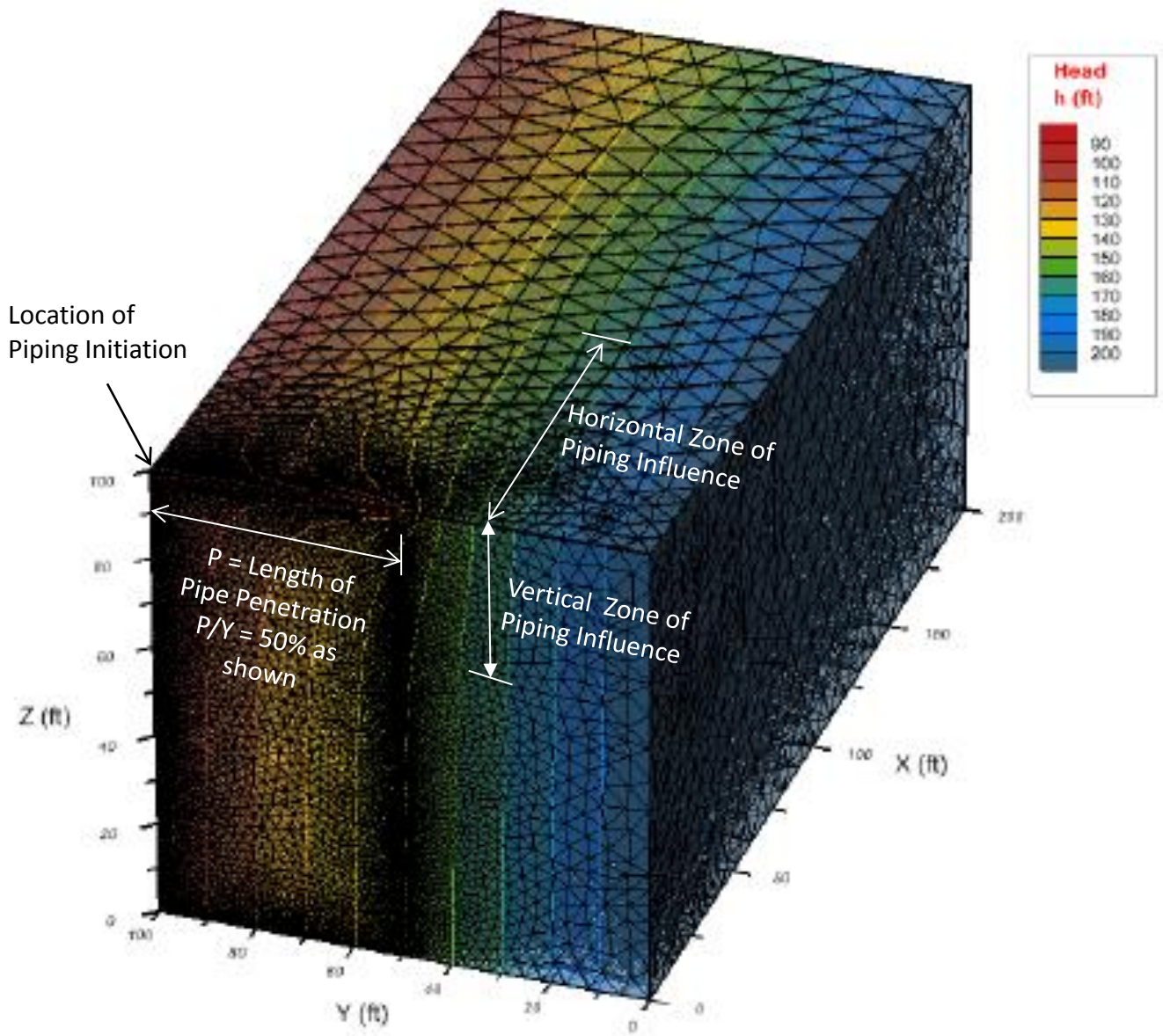


Figure 4. 3-D Seepage Model Configuration

The current 3-D model was prepared using the software program SVFlux 2009 by Soilvision Software. This software can be used for 1-, 2-, and 3-D finite element modeling of seepage. The program uses hp-adaptive meshing to generate the mesh on geometry that the user provides. The adaptive meshing algorithm allows the program to refine the mesh in regions of high gradients in order to more accurately estimate the gradients without the user having to iterate through mesh refinements. Unfortunately the exact recreation of the UF triangular pipe geometry was not possible due to the geometric limitations of the SVFlux software. The pipe was modeled as a

rectangular pipe, with a square profile. The “radius” reported in the current model results is equal to the length of the sides of the square.

The differences observed between the UF and the current research studies is likely a result of the differences in geometry of the pipe and the density of the mesh that could be achieved in the current study as compared to the mesh limitations inherent to the software used in the original study. Based on our comparison of the two different study results, we believe that the gradients reported in the UF study were less than what actually would occur due to averaging across larger elements. The model for the current study uses approximately 70,000 nodes and 50,000 elements. Mesh density in the current study was controlled by the software and parameters controlled by the software which were optimized to assure convergence of the finite element solution.

The current study looked at the influence of the following factors on estimated gradients:

- a. radius of the pipe, R,
- b. depth of the permeable layer beneath the upper confining layer in the model, D,
- c. penetration of the pipe, P, and
- d. anisotropy of the upper permeable layer of material.

Three radii were considered for basic model,  $R = 0.0050 \times L$  (0.5 feet),  $0.0075 \times L$  (0.75 feet) and  $0.0100 \times L$  (1 foot); the basic model comprised of the full depth permeable layer ( $D = Z = 100$  feet) and  $L = Y = 100$  feet. For the remaining models only two radii were considered;  $0.0050 \times L$  (0.5 feet) and  $0.0100 \times L$  (1 foot). In addition to the depth of the permeable layer in the model being set at 100 feet, an analysis was also conducted with the depth of the permeable layer limited to the upper 15 feet immediately below the top confining layer of the model. The penetration of the pipe was varied from 5 percent (5 feet) to 95 percent (95 feet) of the model length Y of 100 feet, generally in steps of 10 percent (10 feet). A single permeable material was used to reduce the complexity of the model. A hydraulic conductivity of 2.8 feet per day (feet/day) ( $1.0 \times 10^{-3}$  centimeters/second) with a saturated volumetric water content of 0.3 was used for the permeable layer. The anisotropy of the material was set to  $k_h/k_v = 1$  for the basic model, with a variation of  $k_h/k_v = 4$  in subsequent study cases. A head of 200 feet was applied uniformly along the upstream face of the model ( $Y = 100$  feet) and a head of 100 feet was applied uniformly along the downstream face of the model ( $Y = 0$  feet) to generate an average gradient of 1.0 in the model. Review boundaries were applied along the faces of the pipe to allow water to flow out of the model, while the remaining boundaries were input as no (zero) flow boundaries

The results for an equivalent 2-dimensional models (at  $X = 0$ ) were compared with the basic 3-D model results, using the same dimensions and properties incorporated in the 3D models.

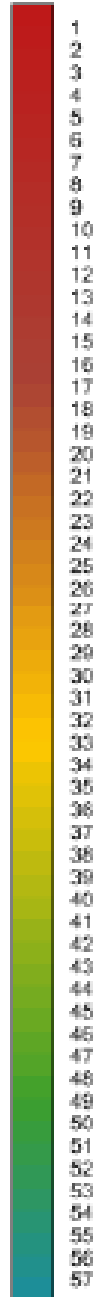


Figure 5.  
Gradient  
Scale

## Modelling Results

The first use of our model results was an examination of the direction and relative magnitude of gradient and flow vectors in the vicinity of the active erosion face (pipehead) as well as in the region between the pipehead and the downstream point of initiation. The direction and magnitude of these vectors in the immediate vicinity of the pipehead will help to inform our understanding of the **detachment** erosion mechanism, whereas, examination of the magnitude of these vectors between the pipehead and the discharge location help to inform our understanding of the **transport** erosion mechanism.

Example results showing gradient contours (see Figure 5 for gradient color scale definition) and velocity (flux) vectors at the  $X = 0$  axis-symmetric boundary of the model with the pipe penetration at 50 feet (50% of the model length along the Y axis) are shown on Figure 6. Gradient contours and velocity (flux) vectors along a cross-section perpendicular to the pipe feature at the pipehead are shown on Figure 7 for the same pipe penetration of 50 feet. The pipe radius in these results is 0.5 feet (6-inches).

Examination of the results illustrated on these example figures and other 3-D modeling results lead to the following conclusions:

- Gradients at, and in the immediate vicinity of the pipehead and along the length of the pipe are very high; e.g.  $> 40$  in the pipehead region to 25 to 30 at the downstream end of the pipe). If an average gradient correction factor of 0.15 to 0.2 is applied to the results, simulating the kind of conditions that would exist in the foundation of most dams and levees under normal maximum hydraulic loading conditions, the estimated 3-D gradients would be at least 6 to 8 in the pipehead region and 4 to 6 along the remainder of the pipe). Hence the model results suggest that the 3-D influence of the pipe reinforces that the gradients are sufficient from the time of initiation through full penetration of the pipe to **detach** a range of soil particles during the piping process.
- The direction of the gradient vectors (the same as velocity/flux vectors) at the pipehead is highly variable ranging from horizontal at the top of the pipe adjacent to the “confining” top layer, to vertical along the base of the pipe along the pipe axis. Vertical gradients appear to range from greater than 20% higher to approximately equal to the horizontal gradients in the pipehead area.

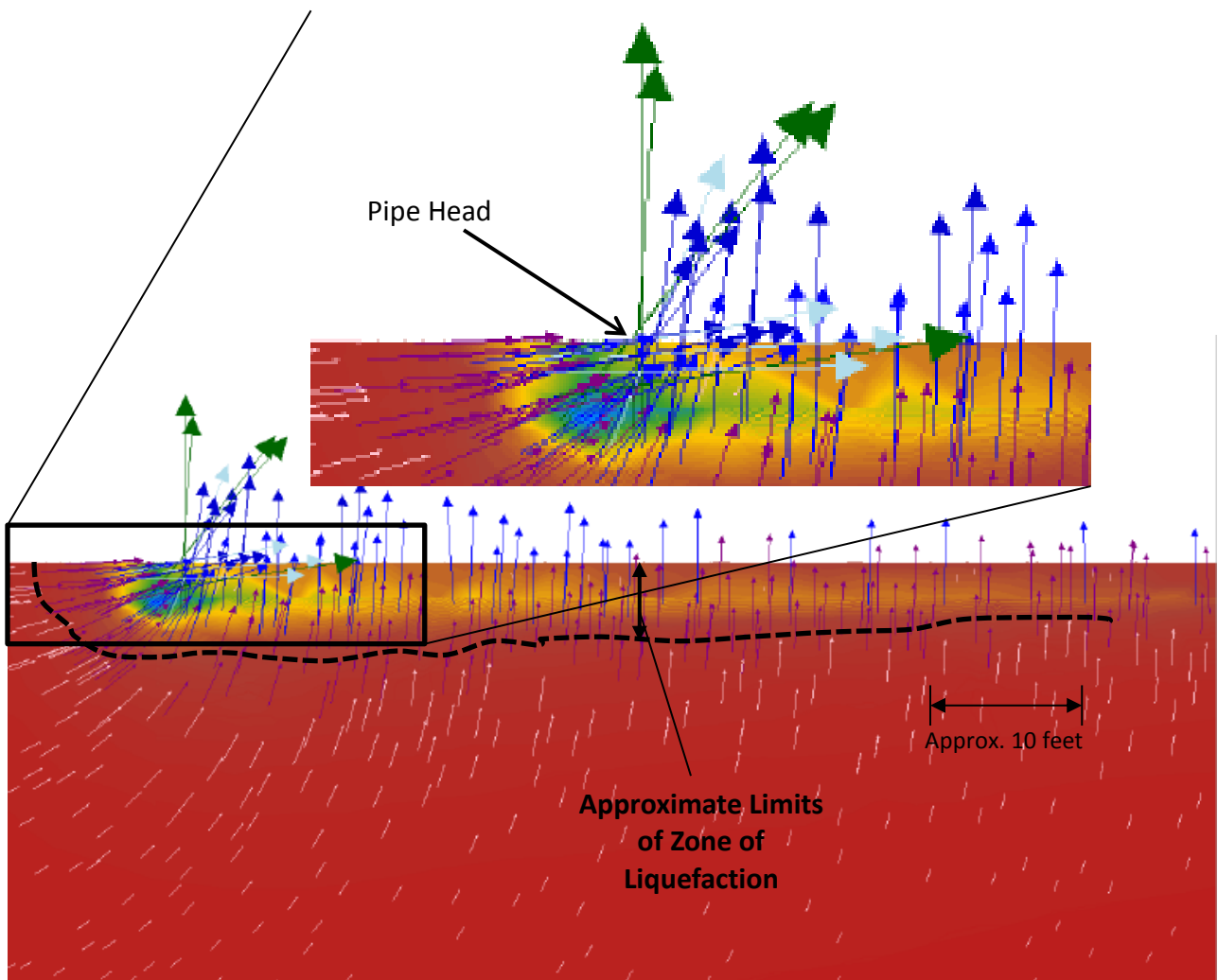


Figure 6. Example Gradient/Flux Vectors Entering Pipe Head Parallel to Pipe ( $X = 0$ ); Pipe Head at 50% Penetration ( $Y = 50$  Feet)

- The gradient and velocity (flux) vectors along the axis of the pipe become essentially vertical within about 10 to 20 pipe radii downstream from the pipe head.
- The horizontal zone of 3-D influence of the erosion feature is a maximum of about 80 radii similar to the findings by Schmertmann.
- The vertical zone of 3-D influence of the erosion feature is approximately comparable to the depth of pipe penetration when the permeable layer is the full height of the model. The vertical zone of 3-D influence is essentially the entire layer when the layer depth is less than the amount of pipe penetration.

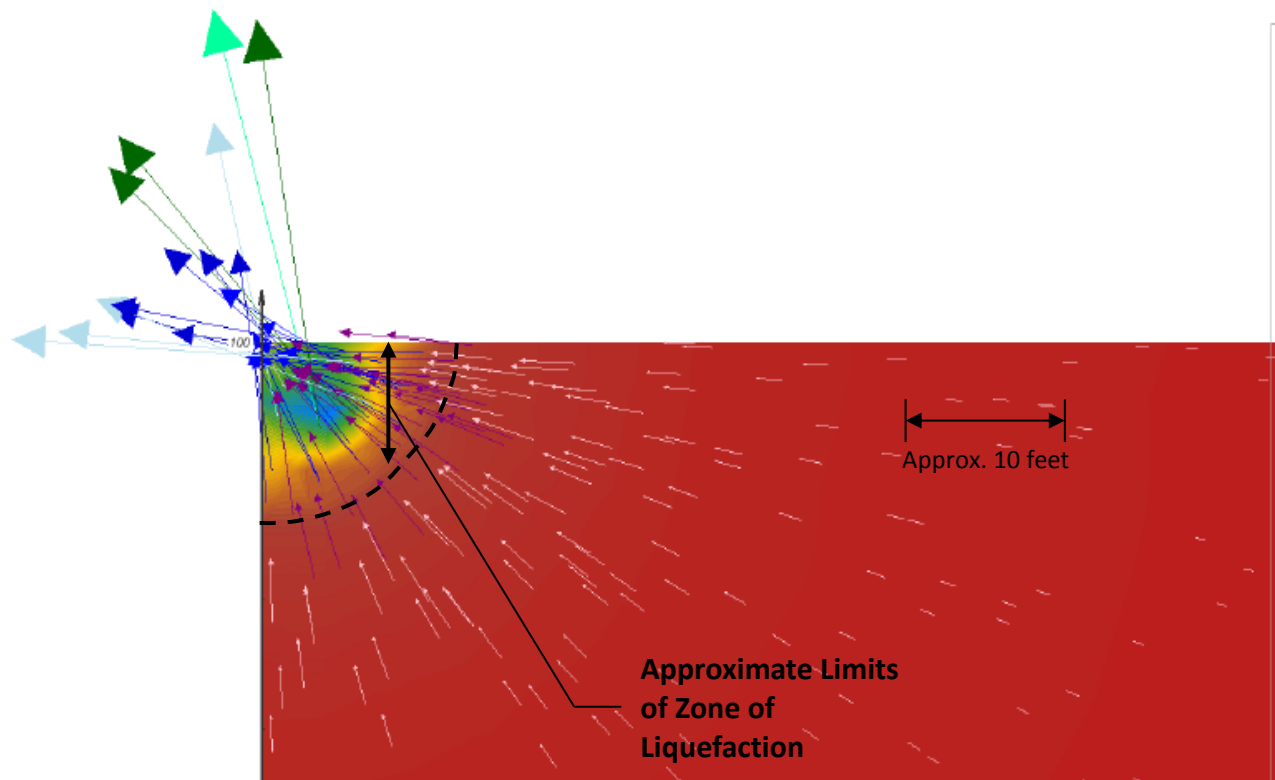


Figure 7. Example of Gradient/Flux Vectors Entering Pipe Head Area Perpendicular to Pipe; 50% Pipe Penetration (Y = 50 Feet)

- Vertical gradients are substantially higher than 1.0 for more than 70 to 80% of the length of the pipe even when a correction factor of 0.2 is applied to the computer model results. These model results suggests that a zone of disturbance (liquefaction) around the perimeter of the pipe as postulated by Schmertmann. This zone of disturbance may extend as much as 10 to 20 radii around the pipe. For a 3-inch radius, the zone of disturbance may range for a radius of 30 to 60 inches. For a 6-inch radius, the zone may range for a radius ranging from 5 to 10 feet. The result of this occurrence suggests that upward (near vertical) gradients and velocity vectors would have a significant influence on the **transport** of particles in the pipe once **detachment** has occurred in the pipehead area. This observation is consistent with Schmertmann’s observation noted above: “the flow velocity needed for the piping process is substantially less that the flow velocity required in a concentrated leak to cause “scour” (concentrated leak erosion)” such as those presented by Briaud (2007). However, as vertical gradients and upward flows decrease near the downstream end of the pipe, there may be a heightened potential for deposition to influence the pipe development process.

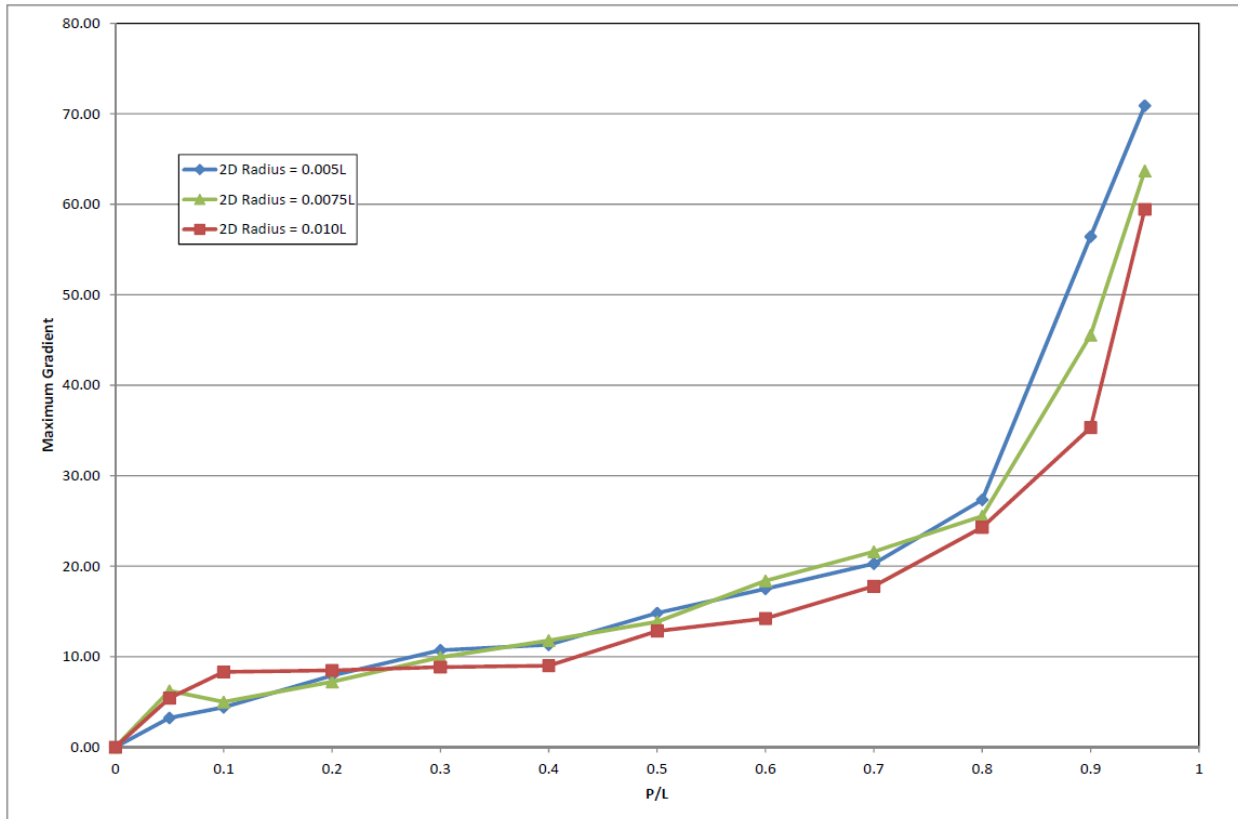


Figure 8. Summary of Estimated 2-D Gradients at the Pipehead as a Function of Pipe Penetration into the Model

Figures 8 through 10 contain a summary of the estimated 2-D versus 3-D gradients at the pipehead, and total flux from the discharge end of the piping feature as a function of the piping penetration  $D/L$  (where  $D$  is the penetration length and  $L$  is the total length (100 feet) of the model along the y-axis shown on Figure 5). The computer program SVFlux provides both the 3-D and 2-D results for these comparisons. Note that the results shown on Figure 10 have not been corrected for the axis-symmetric condition of the model. Actual seepage values shown on this figure are 2 times greater.

A number of the study case results are included on these Figures representing 1) various pipe diameters as a function of the y-axis length ( $L$ ), 2) for permeable layer depths of 15 feet (labeled as shallow) and 100 feet (no label other than the pipe radius) and for a shallow layer when the anisotropy ratio is changed from 1 to 4 ( $k_h/k_v$ ).

Table 3 contains a summary of the average differences in the estimated gradients between the 2-D and 3-D models for the case of:

- $R = 0.005L$  (6-inches)
- Shallow permeable layer (15 feet below the upper confining layer at  $A = 100$  feet)
- Anisotropy Ratio of 1

The results shown in Table 3 can be roughly compared to the results of previous 2-D evaluations of seepage conditions along the Borel Conduit beneath the Isabella Auxiliary Dam (Ferguson, 2012) by comparing the results in column 3 with the noted gradients summarized in the comment column.

Table 3. Comparison of 2-D versus 3-D Gradients at Pipehead

P/L	Est. Max.2-D Gradient in Model	Est. Max 2-D Gradient with Correction Factor of 0.2 applied	Est. Max 3-D Gradient in the Model <sup>1</sup>	Est. Max 3-D Gradient with Correction Factor of 0.2 applied <sup>2</sup>	Ratio of Corrected 3-D to 2-D Gradients	Comments
0	0.00	0.0	8.14	1.6	> 16	
0.05	3.24	0.6	12.56	2.5	3.88	
0.1	4.41	0.9	20.70	4.1	4.69	(2-D $i=0.4$ ) <sup>3</sup>
0.2	7.90	1.6	32.38	6.5	4.10	
0.3	10.71	2.1	43.66	8.7	4.08	(2-D $i=0.5$ ) <sup>3</sup>
0.4	11.32	2.3	67.98	13.6	6.01	Point of maximum 3-D effect
0.5	14.82	3.0	66.69	13.3	4.50	(2-D $i=0.8$ ) <sup>3</sup>
0.6	17.50	3.5	83.65	16.7	4.78	
0.7	20.27	4.1	116.60	23.3	5.75	3-D gradients become more erratic at this penetration
0.8	27.34	5.5	129.70	28.5	5.22	(2-D $i=0.9$ ) <sup>3</sup>
0.9	56.43	11.3	162.10	32.4	2.87	3-D effect diminishes at 90%
0.95	70.90	14.2	199.40	39.9	2.81	

- Notes:
- <sup>1</sup> The gradients shown in this column represent the Model estimated concentration factors based on an applied average gradient,  $i_{ave} = 1.0$  across the y-axis.
  - <sup>2</sup> The gradients shown in this column represent an approximate concentration factor that would be expected for a model with an applied average gradient,  $i_{ave} = 0.2$  applied across the y-axis.
  - <sup>3</sup> These are the estimated 2-D gradients reported for Isabella Auxiliary Dam in Ferguson, 2012 estimated with Seep/W for comparison with the SVFlux results

The authors attribute the difference between the 2-D estimated gradients with the two different computer programs to two primary factors: 1) the estimated maximum gradients from the SVFlux 2-D analyses in this table are typically at the lower corner of the pipehead and include both x and y components, and 2) the SVFlux adaptive meshing generated a much finer mesh at the pipehead and hence higher 2-D estimated gradients. This comparison hints at the uncertainties associated with 2-D seepage analyses methods.

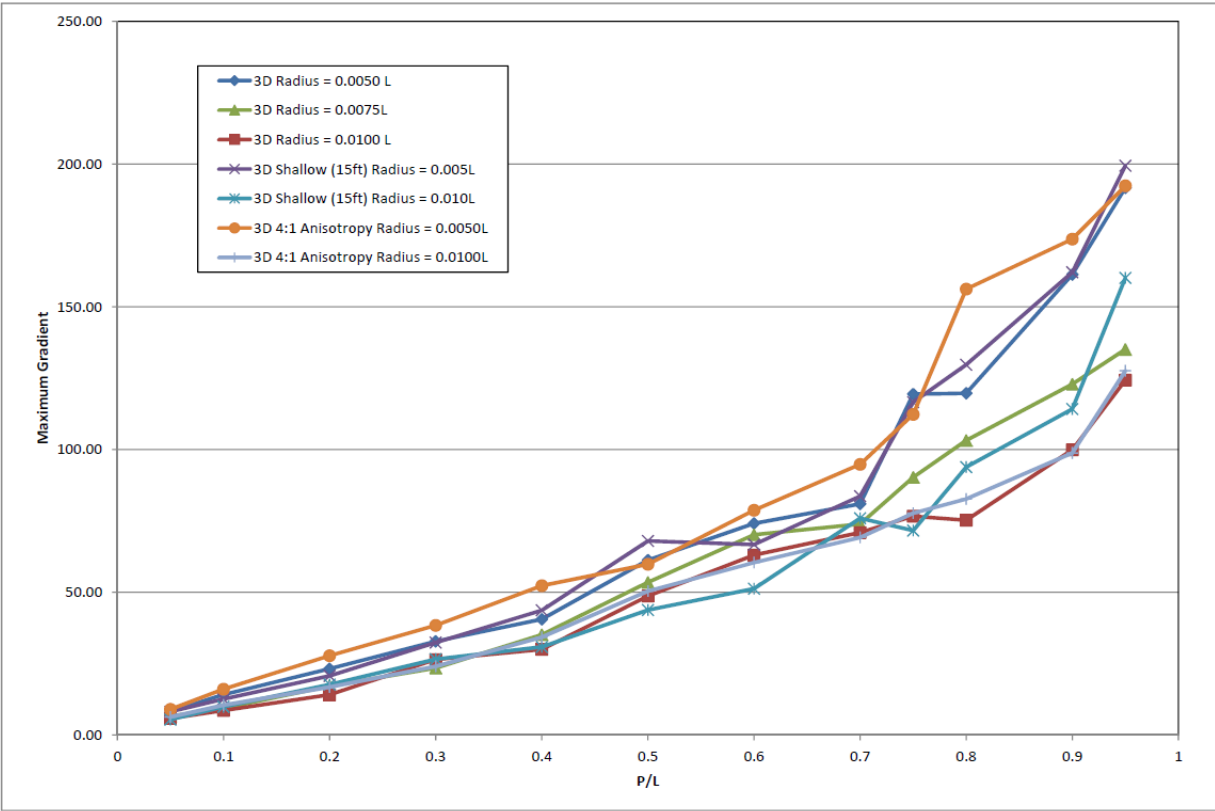


Figure 9. Summary of Estimate 3-D Gradients at the Pipehead as a Function of Pipe Penetration into the Model

Table 4 contains a summary of the estimated flux (flow) through all surfaces of the pipe for both the 2-D and 3-D conditions. for the case of:

- R = 0.005L (6-inches)
- Shallow permeable layer (15 feet below the upper confining layer at A = 100 feet)
- Anisotropy Ratio of 1

Note that the results in Table 4 with all correction factors applied, indicated that the total flux discharging from the pipe is about 9 to 17 times greater in the 3-D model verses what is predicted in the SVFlux 2-D model.

The corrected 3-D model results in Table 4 have been set to approximately simulate the maximum average gradient conditions in the foundation of Isabella Auxiliary Dam. The maximum flow quantities observed discharging from a defective toe drain pipe at the Isabella Auxiliary Dam where piping had initiated and was in the process of continuing toward the reservoir ranged from 0 to as much as 8 gpm depending on reservoir level as shown in Figure 11. These observations are generally consistent with the 3-D seepage model results.

Table 4. Summary of Estimated 2-D and 3-D Flux (flow quantity) Values

P/L	Est. Max.2-D Flux in Model (gpm)	Est. Max 2-D Flux with Correction Factor of 0.2 applied <sup>2</sup> (gpm)	Est. Max 3-D Flux in the Model (gpm)	Est. Max 3-D Flux with Correction Factor of 0.4 applied <sup>1</sup> (gpm)	Ratio of Corrected 3-D to 2-D Flux	Comments
0	0	0	0.16	0.07	> 0.3	
0.05	0.16	0.04	0.48	0.19	6.20	
0.10	0.23	0.08	1.39	0.55	12.24	
0.2	0.40	0.14	2.67	1.07	13.44	
0.3	0.57	0.20	4.74	1.90	16.71	
0.4	0.73	0.27	5.92	2.37	16.26	
0.5	0.94	0.35	7.84	3.14	16.64	
0.6	1.17	0.44	10.10	4.04	17.28	Point of max 3-D effect
0.7	1.47	0.55	11.62	4.65	15.81	
0.8	1.89	0.72	14.91	5.96	15.77	
0.9	2.61	0.99	17.03	6.81	13.03	
0.95	3.41	1.28	19.69	7.88	11.57	

Notes: <sup>1</sup> This is a net correction factor which is the product of the average gradient correction of  $100/500 = 0.2 \times 2$ . The second factor of 2 is applied to compute the total flux from the axis-symmetric model that includes only  $\frac{1}{2}$  of the piping defect.

<sup>2</sup> This is corrected gradient estimated by applying the average gradient correction of 0.2 to the results of the pipe with a radius of 1 foot.

## CONCLUSIONS AND RECOMMENDATIONS

This paper has presented a review of the primary considerations related to internal erosion and the development of piping features that can lead to the development of a seepage failure mode. Three-dimensional influences have been long been suspected to be a significant factor in the internal erosion process but until recently, sufficient computer modeling tools were not widely available to allow for a deeper examination to inform our understanding of these 3-D effects. A state-of-the-art 3-D model using the computer program SVFlux has been developed and presented as part of this paper. The model replicates the initial work completed at the University of Florida but with substantially enhanced meshing and graphical output capabilities.

The initial results of the 3-D modeling work confirm many of the insights presented by Schmertmann and allow for an in-depth examination of the internal erosion process. While much still remains to be learned, the following general conclusions can be made.

1. Unfiltered geologic and/or man-made defects are a primary consideration in the assessment of “initiation”. The 3-D model results suggest that the concentration of

gradients and flows around defects is significant and likely provides the energy required to initiate the erosion process. Finding such defects is critical to the assessment of potential failure modes, estimating the probability of initiation, and in the overall seepage safety of a structure.

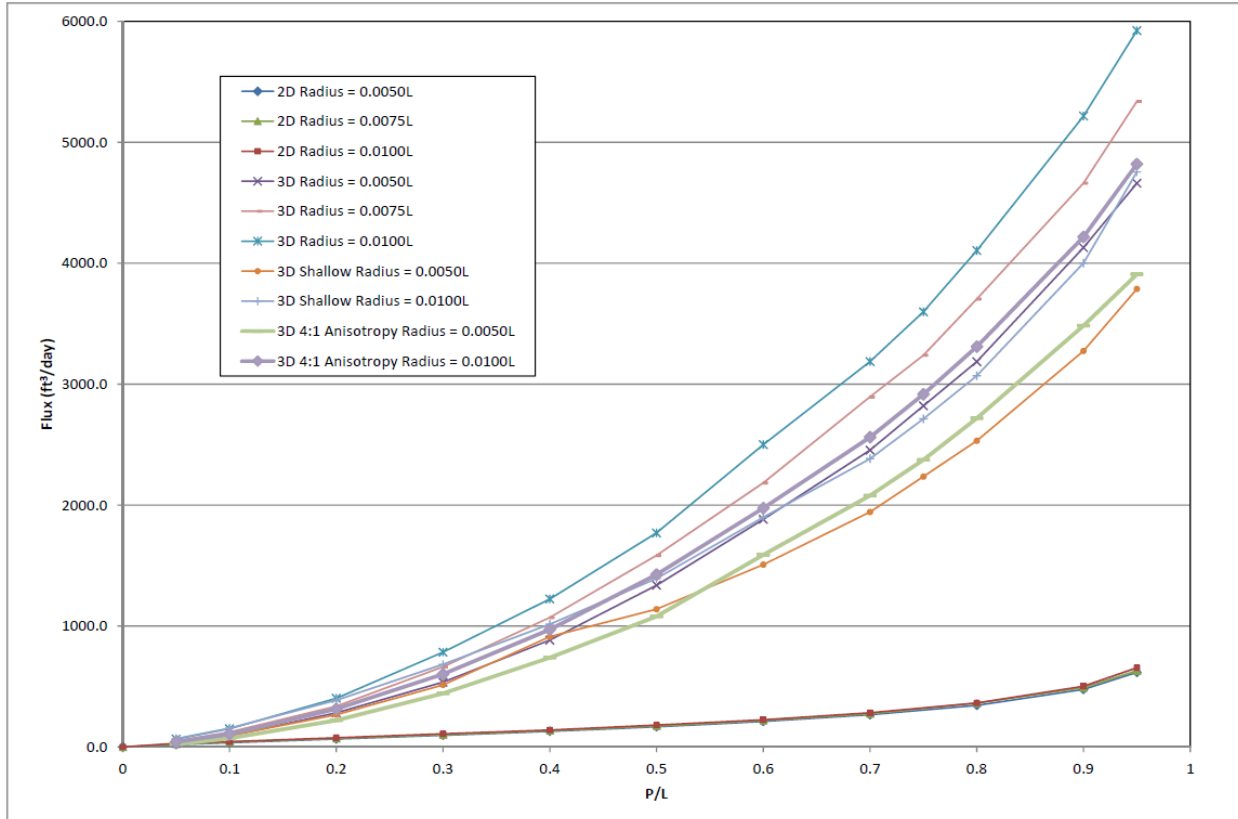


Figure 10. Summary of Estimated 2-D and 3-D Total Flux into the Pipe as a Function of Pipe Penetration into the Model

2. Once initiated, gradients at the active front (pipehead) will be sufficient for the entire length of a potential erosion pathway to sustain an erosion process. Results of the 3-D analyses confirm that the key considerations for the estimation of the potential for a piping failure are:
  - ✓ The potential for a continuous pathway (layer, crack, hydraulic fracture or other natural or man-made defect from the point of initiation to the reservoir or water source
  - ✓ The permeability of the soils and ability to generate adequate seepage quantity and velocity (energy) to **detach and transport** the full range of soil particle sizes along the pathway
  - ✓ The erodibility of the soils along the pathway (coefficient of uniformity,  $C_u$ ; plasticity, density/specific gravity)
  - ✓ Conditions that promote the stability of the piping feature (roof or pipe channel)

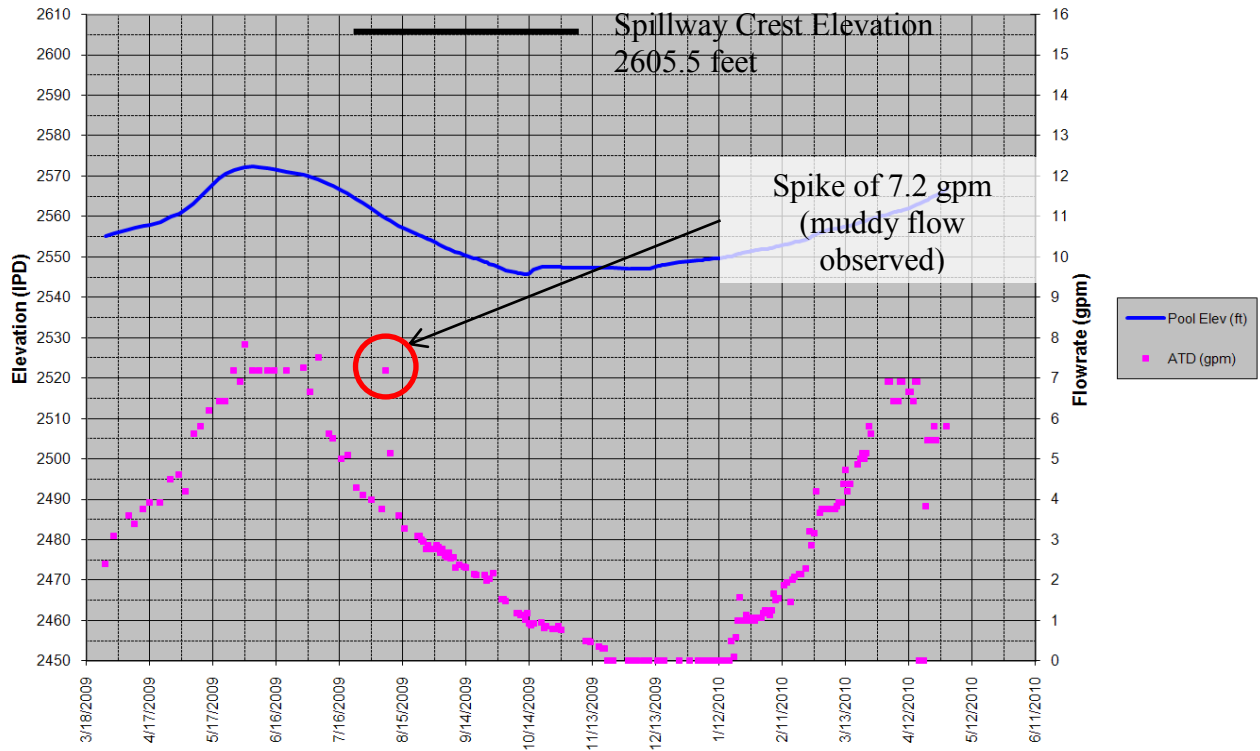


Figure 11 – Plot of Seepage Discharging from Defective Isabella Auxiliary Dam Drain Pipe

- ✓ Conditions that could arrest the advancement of the piping/erosion feature such as changes in material type along the pathway, collapse, and development of a natural filter. Natural filters may develop in the presence of more widely graded soils and sufficient energy only to transport a portion of the gradation, leaving coarse materials deposited in the pipe that eventually cause a natural filter to develop.
- 3. Transport of detached particles will be significantly influenced by vertical seepage gradients for the majority (75 to 80%) of the pipe length that has developed.
- 4. A significant zone of disturbance or liquefaction likely develops in the region surrounding a pipe. This phenomenon could cause a very rapid gross enlargement process and also contribute to localized instability such as observed at the downstream toe of Big Bay dam at the onset of the gross enlargement process.

#### REFERENCES

1. Briaud, J-L, Case Histories in Soil and Rock Erosion, 9<sup>th</sup> Peck Lecture, February 12, 2007.
2. Donahue, C., Critical Gradient for Internal Erosion in Earthen Dams: A Comparative Analysis of Two Predictive Methodologies, Master of Engineering Thesis, Massachusetts Institute of Technology, June 2013.
3. Federal Emergency Management Agency (FEMA), Technical Manual: Conduits through Embankment Dams, FEMA 484CD, September, 2005.

4. Fell, R., Wan, C. F., Cyganiewicz, J., and M Foster, Time for Development of Internal Erosion and Piping in Embankment Dams, Journal of Geotechnical and Geoenvironmental Engineering, ASCE, April 2003, pp 307- 314.
5. Ferguson, K.A., Investigation and Evaluation of Seepage Conditions Around Outlet Conduits – Two Case Histories, Presentation at the Ohio River Valley Soil Seminar (ORVSS), Louisville, KY, October 20, 2010.
6. Ferguson, K.A., Investigation and Evaluation of Seepage Conditions and Potential Failure Modes Around Outlet Conduits, Proceedings of the 2012 Annual Conference, United States Society on Dams (USSD), New Orleans, LA, April, 2012.
7. Ferguson, K.A., Soudkhah, M., and E. Sossenkina, Potential for Cracking around Outlet Conduits and Its Impact on Seepage Safety, Proceedings of the 2013 Annual Conference, United States Society on Dams (USSD), Phoenix, AZ, February, 2013.
8. Ferguson, K.A., Anderson, S., and E. Sossenkina, Reexamination of the 2004 Failure of Big Bay Dam, Mississippi, Proceedings of the 2014 Annual Conference, United States Society on Dams (USSD), San Francisco, CA, April 2014.
9. Goodman, R. E., Karl Terzaghi, The Engineer as Artist, ASCE press, 1999, page 266.
10. Halpin, E., and K. Ferguson, US Army Corps of Engineers Dam Safety Program Status and Lessons in Transitioning to Risk Informed Approaches, ASDSO Journal of Dam Safety, Vol 2, Spring 2007, pp 24-36.
10. Hjulstrom, F., Doctoral Thesis, “Studies of the Morphological Activity of Rivers as Illustrated by the River Fyris”, Bulletin Mineral Geol. Inst. University of Uppsala, 25: 221-528, 1935.
11. International Commission on Large Dams (ICOLD), Internal Erosion of Existing Dams, Levees and Dikes, and Their Foundation, Bulletin 164, Volume 1: Internal Erosion Processes and Engineering Assessment, 2013.
12. Ishbash, S. V. 2<sup>nd</sup> Conference on Large Dams, Vol, V, 1936.
13. McCook, D.K., and K.O. Grotrian, Using SIGMA/W to Predict Hydraulic Fracture in an Earthen Embankment, Proceeding of the Annual Conference, Association of State Dam Safety Officials, Seattle, WA, 2010.
14. Perzmaier, S., “Hydraulic Criteria Focusing Critical Gradient and Flow Velocity (cohesionless soils)”, Annual Meeting of the European Working Group on Internal Erosion in Embankment Dams, Stockholm, Sweden, September, 2006.
15. Schmertmann, J.H., “The Non-filter Factor of Safety Against Piping Through Sand”, ASCE Geotechnical Special Publication No. 111, Judgment and Innovation, F. Silva and E Kavazanjian, eds., ASCE, Reston, VA, 65-132, 2000.
16. Selljeyer, J.B., On the Mechanism of Piping Under Impervious Structures, *Doctorate Dissertation*, Technical University Delft, 1988.
17. Sherard, J.L., Hydraulic Fracturing in Embankment Dams, American Society of Civil Engineers (ASCE) Journal of Geotechnical Engineering, October, 1986 (First presented at the ASCE Spring Convention held in Denver, CO, 1985).
18. Sherard, J.L., Dispersive Soils

19. Townsend, F.C., Schmertmann, J.H., Logan, T.J., Pietrus, T.J., and Y.W. Wong, An Analytical and Experimental Investigation of a Quantitative Theory for Piping in Sand, Final Report, University of Florida, 1981.
20. Townsend, F.C., Bloomquist, D., Shiau, J-M, Martinex, R. and H. Rubin, Analytical and Experimental Evaluation of Piping and Filter Design for Sands, Report to the U.S. Bureau of Reclamation, University of Florida, Depart. Of Civil Engineering, January, 1988.
21. Tracy, F.T., “Three-Dimensional Finite Element Program for Steady-State and Transient Seepage Problems”, U.S. Army Waterways Experimental Station, Automatic Data Processing Center, Vicksburg, Mississippi.
22. U.S. Army Corps of Engineers (Corps), ER 1110-2-1156, Safety of Dams – Policy and Procedures, October 28, 2011.
23. U.S. Bureau of Reclamation and the U.S. Army Corps of Engineers, Best Practices in Dam and Levee Safety Risk Analysis, 3 December 2012.
24. Van Beek, V., Yao, Q. Van, M., and F. Barends, “Validation of Sellmeijer’s model for backward piping under kikes on multiple sand layers, ICSE6, Paris, France, August 27-31, 2012, pp 543 – 550.
25. Vandenboer, K., van Beek, V., and A Bezuijen, 3D finite element method (FEM) simulation of groundwater flow during backward erosion piping, *Front. Struct. Civil Engineering*, Vol 8(2), 2014, pp 160-162.
26. Wong, Y.W., Three Dimensional Finite Element Analysis of a Quantitative Piping Theory, Report Presented to the Department of Civil Engineering at the University of Florida in Partial Fulfillment of the Requirements for the Degree of Master of Engineering, August, 1981.